Opto-Thermal Properties of Fibers. XI. The Effect of Thermal Annealing of Drawing Behavior for Egyptian Polyester Fibers on the Crystallinity and Some Optical Parameters

A. A. HAMZA, I. M. FOUDA, M. A. KABEEL, E. A. SEISA, F. M. EL-SHARKAWY

Physics Department, Faculty of Science, Mansoura University, Mansoura, Egypt

Received 6 August 1996; accepted 18 November 1996

ABSTRACT: The structure developed of annealed Egyptain poly(ethyleneterephthalate) (PET) fibers is studied interferometerically due to the drawing process. Using a two-beam Pluta polarizing interference microscope connected to a device to dynamically study the draw ratio with the birefringence changes, the relations of drawing changes with some optical parameters are given. The evaluation of density, the mean square density fluctuation $\langle \eta^2 \rangle$, crystallinity, amorphous orientation, crystalline orientation functions, number of chains per unit volume N_e, and number of random links between the network junction points N has been found. The results obtained clarify the effect of annealing time and temperature with different draw ratios on the structure of PET fibers. Empirical formula is suggested to correlate the changes in f_θ, θ, Δn_a, and A with the draw ratio. Microinterferograms and curves are given for illustration. © 1998 John Wiley & Sons, Inc. J Appl Polym Sci 68: 1371–1386, 1998

INTRODUCTION

Polyester fibers are among the most important synthetic textile fibers. Work is found in the literature concerning the various types of modifications of these fibers either via physicomechanical or chemical processes in order to attain more favorable properties.[1–6] By extrusion is meant the formation of filament directly from the melt and by drawing the further elongation of the solid crystalline extruded material. In the course of fiber manufacture, the molten polymer is first extruded through holes of required diameters, and the solidifying filaments are wound up on rollers. The product obtained in this way is then drawn further in order to arrive at the final yarn. Usually, no crystallite orientation is found in the extruded filament. Occasionally observed weak birefringence effects have been interpreted as being due to some incipient orientation in the amorphous portions of the molecules. In the case of high wind-up speeds, orientation can occur; according to the earlier findings, this orientation is an imperfect version of the final fiber, as if an incomplete drawing had taken place.[7]

The degree of orientation could vary significantly from one fiber to another, depending on the fiber history during manufacture and subsequent processing operations.

This article presents some mechanical and optical properties for annealed PET fibers at different conditions to investigate the types of modifications and changes in the internal structure due to external effects.

THEORETICAL CONSIDERATION

The Pluta polarizing interference microscope[8,9] connected to a device to dynamically study the draw ratio was used in the present work to determine the refractive indices of drawn and undrawn for annealed fibers, where

$$n_a^{\parallel} = n_L + (\lambda/h)\cdot(E^{\parallel}/A) \qquad (1a)$$

Correspondence to: I. M. Fouda.

Journal of Applied Polymer Science, Vol. 68, 1371–1386 (1998)
 CCC 0021-8995/98/091371-16

Table I(a) Values of F_c, F_a, and χ at 120°C and 2 h

Draw Ratio	$\chi \times 10^{-4}\%$	F_c	$\langle\eta\rangle^2 \times 10^{-2}$	F_a	ρ
1.000	41.11	—	0.355	0.6052	1.386
1.167	36.48	0.1642	0.339	0.5543	1.380
1.333	33.38	0.3133	0.326	0.4912	1.376
1.500	32.86	0.4419	0.323	0.4824	1.376
1.667	34.93	0.5477	0.333	0.5304	1.378
1.833	32.35	0.6323	0.320	0.5322	1.375
2.000	34.93	0.7000	0.333	0.5824	1.378
2.167	37.51	0.7536	0.343	0.5517	1.381
2.333	31.83	0.7959	0.318	0.5935	1.375
2.500	33.38	0.8298	0.326	0.6444	1.376

$$n_a^{\perp} = n_L + (\lambda/h)\cdot(E^{\perp}/A) \qquad (1b)$$

and

$$\Delta n_a = \frac{\Delta E \lambda}{hA} \qquad (2)$$

where $n_a^{\parallel}$ and $n_a^{\perp}$ are the mean refractive indices of the fiber for light vibrating parallel and perpendicular to the fiber axis, respectively; n_L is the refractive index of the immersion liquid, $E^{\parallel}$ and $E^{\perp}$ are the area of the fiber enclosed under the fringes shift as it crasses of the fiber, h is the interference fringe spacing corresponding to the monochromatic light of wavelength λ, and A is the mean cross sectional area of the fiber. Also, Δn_a is the mean birefringence of the fiber and $\Delta E = (E^{\parallel} - E^{\perp})$ is the area enclosed under the fringe shift using nonduplicated image of the fiber. The axial orientation is expressed by the usual birefringence $\Delta n_a = n_a^{\parallel} - n_a^{\perp}$. *The values of* $n_a^{\parallel}$, $n_a^{\perp}$, Δn_a for PET fiber are given in Table II(a)–(f). From this axial birefringence, the amorphous orientation F_a has been calculated by combining the two-phase model of Samuels[10] and the Gaylord model for crystalline orientation, F_c; the Gaylord model is in good agreement with experimental data on PET, as follows[11]:

$$\Delta n_a = \chi \Delta n_{c^o} F_c + (1 - \chi)\Delta n_{a^o} F_a \qquad (3)$$

with χ = degree of crystallinity, $\Delta n_{c^o} = 0.22$, $\Delta n_{a^o} = 0.27$, and $F_c = (DR^3 - 1)/(DR^3 + 2)$, where DR = draw ratio.

The value of F_a and F_c for PET fiber are given in Table I(a)–(f).

DENSITY

The densities of the samples were estimated with the average refractive index obtained by two-beam interferometric technique. For PET, deVries et al.[12] found a linear relation between the density, as follows:

$$\rho = 4.047(\bar{n}^2 - 1)/(\bar{n}^2 + 2) \qquad (4)$$

with ρ expressed in g/cm^3. This relation is inde-

Table I(b) Values of F_a, F_c, and χ at 140°C and 2 h

Draw Ratio	$\chi \times 10^{-4}\%$	F_c	$\langle\eta\rangle^2 \times 10^{-2}$	F_a	ρ
1.000	42.24	—	0.357	0.6686	1.387
1.160	34.00	0.1575	0.328	0.5858	1.377
1.320	29.61	0.3023	0.305	0.5450	1.372
1.480	29.35	0.4277	0.304	0.5352	1.372
1.640	27.95	0.5321	0.295	0.5233	1.370
1.800	30.85	0.6170	0.312	0.5597	1.373
1.960	29.71	0.6852	0.306	0.5723	1.372
2.120	30.33	0.7398	0.309	0.6349	1.373
2.280	29.24	0.7834	0.303	0.6367	1.371
2.440	27.12	0.8185	0.289	0.6475	1.369

Table I(c) Values of F_c, F_a, and χ at 160°C and 2 h

Draw Ratio	$\chi \times 10^{-4}\%$	F_c	$\langle\eta\rangle^2 \times 10^{-2}$	F_a	ρ
1.000	52.40	—	0.365	0.9167	1.399
1.160	48.30	0.1575	0.366	0.8178	1.394
1.320	46.76	0.3023	0.365	0.7165	1.393
1.480	50.35	0.4277	0.366	0.7663	1.397
1.640	50.35	0.5321	0.366	0.7695	1.397
1.800	48.81	0.6170	0.366	0.7583	1.395
1.960	47.79	0.6852	0.365	0.7728	1.394

Table I(d) Values of F_c, F_a, and χ at 120°C and 4 h

Draw Ratio	$\chi \times 10^{-4}\%$	F_c	$\langle\eta\rangle^2 \times 10^{-2}$	F_a	ρ
1.000	49.07	—	0.366	0.7140	1.395
1.160	45.22	0.1575	0.363	0.6036	1.391
1.320	39.77	0.3023	0.351	0.5902	1.384
1.480	42.09	0.4277	0.357	0.6122	1.387
1.640	39.10	0.5321	0.349	0.5878	1.383
1.800	40.49	0.6170	0.353	0.5802	1.385
1.960	39.57	0.6852	0.350	0.5810	1.384
2.120	34.36	0.7398	0.330	0.6026	1.378
2.280	33.85	0.7834	0.328	0.6221	1.377

Table I(e) Values of F_c, F_a, and χ at 140°C and 4 h

Draw Ratio	$\chi \times 10^{-4}\%$	F_c	$\langle\eta\rangle^2 \times 10^{-2}$	F_a	ρ
1.000	45.56	—	0.364	0.7308	1.392
1.160	38.38	0.1575	0.346	0.6067	1.382
1.320	42.14	0.3023	0.357	0.6013	1.387
1.480	43.12	0.4277	0.359	0.5455	1.388
1.640	37.71	0.5321	0.344	0.5281	1.382
1.800	41.47	0.6170	0.355	0.5394	1.386
1.960	42.24	0.6852	0.357	0.5189	1.387
2.120	42.40	0.7398	0.358	0.4924	1.387
2.280	42.81	0.7834	0.358	0.4840	1.388
2.440	41.27	0.8185	0.355	0.4903	1.386

Table I(f) Values of F_c, F_a, and χ at 160°C and 4 h

Draw Ratio	$\chi \times 10^{-4}\%$	F_c	$\langle\eta\rangle^2 \times 10^{-2}$	F_a	ρ
1.000	37.92	—	0.345	0.6818	1.382
1.160	38.18	0.1575	0.346	0.6962	1.382
1.320	37.25	0.3023	0.342	0.6608	1.381
1.480	38.69	0.4277	0.347	0.6720	1.383
1.640	35.65	0.5321	0.336	0.6582	1.379
1.800	35.81	0.6170	0.336	0.6718	1.379
1.960	34.98	0.6852	0.333	0.6833	1.378

Table II(a) Values of n_a'', $n_a^{\perp}$, and Δn_a for PET Fiber at 120°C and 2 h

Draw Ratio	n_a''	$n_a^{\perp}$	Δn_a	n_{iso}	K
1.000	1.666	1.568	0.0980	1.601	0.4335
1.167	1.671	1.561	0.1100	1.598	0.4331
1.333	1.671	1.558	0.1130	1.596	0.4328
1.500	1.676	1.555	0.1210	1.595	0.4327
1.667	1.688	1.551	0.1370	1.597	0.4329
1.833	1.691	1.547	0.1440	1.595	0.4327
2.000	1.702	1.544	0.1580	1.597	0.4329
2.167	1.703	1.546	0.1570	1.598	0.4331
2.333	1.706	1.539	0.1670	1.595	0.4326
2.500	1.715	1.536	0.1790	1.596	0.4328

Table II(b) Values of n_a'', $n_a^{\perp}$, and Δn_a for PET Fiber at 140°C and 2 h

Draw Ratio	n_a''	$n_a^{\perp}$	Δn_a	n_{iso}	K
1.000	1.672	1.566	0.1062	1.601	0.4336
1.160	1.675	1.557	0.1181	1.596	0.4328
1.320	1.677	1.552	0.1252	1.593	0.4324
1.480	1.681	1.549	0.1316	1.593	0.4324
1.640	1.683	1.547	0.1364	1.592	0.4323
1.800	1.693	1.545	0.1483	1.594	0.4326
1.960	1.697	1.542	0.1554	1.593	0.4325
2.120	1.708	1.537	0.1710	1.594	0.4325
2.280	1.709	1.535	0.1743	1.593	0.4324
2.440	1.711	1.532	0.1786	1.592	0.4322

Table II(c) Values of n_a'', $n_a^{\perp}$, and Δn_a for PET Fiber at 160°C and 2 h

Draw Ratio	n_a''	$n_a^{\perp}$	Δn_a	n_{iso}	K
1.000	1.688	1.568	0.1200	1.609	0.4345
1.160	1.694	1.561	0.1330	1.605	0.4341
1.320	1.695	1.559	0.1360	1.604	0.4340
1.480	1.708	1.556	0.1520	1.607	0.4343
1.640	1.716	1.552	0.1640	1.607	0.4343
1.800	1.721	1.548	0.1730	1.606	0.4342
1.960	1.727	1.544	0.1830	1.605	0.4341

Table II(d) Values of n_a'', $n_a^{\perp}$, and Δn_a for PET Fiber at 120°C and 4 h

Draw Ratio	n_a''	$n_a^{\perp}$	Δn_a	n_{iso}	K
1.000	1.673	1.573	0.1000	1.606	0.4342
1.160	1.674	1.568	0.1066	1.603	0.4338
1.320	1.683	1.558	0.1242	1.600	0.4333
1.480	1.693	1.556	0.1371	1.601	0.4336
1.640	1.696	1.551	0.1442	1.599	0.4333
1.800	1.700	1.550	0.1499	1.600	0.4334
1.960	1.704	1.548	0.1562	1.600	0.4333
2.120	1.706	1.541	0.1647	1.596	0.4329
2.280	1.710	1.539	0.1715	1.596	0.4328

Table II(e) Values of n_a'', $n_a^{\perp}$, and Δn_a for PET Fiber at 140°C and 4 h

Draw Ratio	n_a''	$n_a^{\perp}$	Δn_a	n_{iso}	K
1.000	1.676	1.568	0.1074	1.604	0.4340
1.160	1.676	1.560	0.1161	1.599	0.4332
1.320	1.684	1.560	0.1237	1.601	0.4336
1.480	1.686	1.560	0.1259	1.602	0.4336
1.640	1.688	1.554	0.1346	1.599	0.4332
1.800	1.696	1.553	0.1431	1.601	0.4335
1.960	1.699	1.553	0.1461	1.601	0.4336
2.120	1.700	1.553	0.1470	1.602	0.4336
2.280	1.702	1.552	0.1499	1.602	0.4336
2.440	1.703	1.550	0.1535	1.601	0.4335

Table II(f) Values of n_a'', $n_a^{\perp}$, and Δn_a for PET Fiber at 160°C and 4 h

Draw Ratio	n_a''	$n_a^{\perp}$	Δn_a	n_{iso}	K
1.000	1.676	1.560	0.1164	1.599	0.4332
1.160	1.687	1.555	0.1316	1. 99	0.4332
1.320	1.691	1.552	0.1388	1.598	0.4331
1.480	1.699	1.549	0.1497	1.599	0.4333
1.640	1.703	1.544	0.1582	1.597	0.4330
1.800	1.709	1.542	0.1672	1.597	0.4330
1.960	1.713	1.438	0.1749	1.597	0.4329

pendent of the degree of crystallinity χ and the level of orientation. We calculate the average refractive index as the isotropic refractive index from the following equation[13]:

$$n_{iso} = (n_a^{\parallel} + 2n_a^{\perp})/3 \quad (5)$$

From eqs. (4) and (5), the constant K for different draw ratio at different annealing conditions by using the well-known Gladeston Dala equation can be calculated as follows:

$$K = (n_{iso} - 1)/\rho \quad (6)$$

The results are shown in Table I(a)–(f), which indicate that the constant K varies with different draw ratios at different annealing conditions.

DEGREE OF CRYSTALLINITY

The degree of crystallinity χ was determined by the relation

$$\chi = (\rho - \rho_a)/(\rho_c - \rho_a) \quad (7)$$

with $\rho_c = 1.457$ gm/cm^3 and $\rho_a = 1.336$ gm/cm^3.[11]

Volume fraction of amorphous material was determined by the relation

$$1 - \chi = 1 - (\rho - \rho_a)/(\rho_c - \rho_a) \quad (8)$$

where χ is the volume fraction of crystallinity material.

THE MEAN SQUARE DENSITY FLUCTUATION

For drawn and undrawn PET fiber, the mean square density fluctuation $\langle \eta^2 \rangle$ can be calculated from the following equation[14]:

$$\langle \eta^2 \rangle = (\rho_c - \rho_a)^2 \chi(1 - \chi) \quad (9)$$

The value of ρ, χ, $(1 - \chi)$, and $\langle \eta^2 \rangle$ for PET fiber are given in Table II(a)–(f).

The optical orientation function was defined first by Hermans[15] as

$$f_\theta = (n_a^{\parallel} - n_a^{\perp})/(n_x - n_z) = \Delta n/\Delta n_{\max} \quad (10)$$

where n_x and n_z are the refractive indices parallel and perpendicular to the fiber axis, respectively,

for the ideal fiber. Δn is the measured birefringence, and $\Delta n_{\max}$ is the maximum birefringence for fully oriented fiber. This function takes the values $+1$, 0, $-\frac{1}{2}$, according to the state of orientation perfect, random, or perpendicular to the fiber axis, respectively. A theoretical model exists for molecular reorientation developed by stretching.[16,17] This model considers that the optical anisotropic results from the orientation of anisotropic structural units and the optical properties of these units are identical to those for the ideal fiber. Also, this model, named the aggregate model, gives the partially oriented fiber birefringence Δn_a as

$$\Delta n_a = (\tfrac{1}{2})\Delta n_{\max}(\overline{3\cos^2}\theta - 1) \qquad (11)$$

where θ is the angle between the axis of the unit and the fiber axis (or draw direction), and $\cos^2\theta$ is the average value of $\overline{\cos^2}\theta$.

An empirical formula is suggested to evaluate the relationship between orientation function, orientation angle, area of cross section, and birefringence with the draw ratio, as follows:

$$\ln[f(\theta)\Delta n/A\theta] = CR + Y \qquad (12)$$

where C and Y are constants characterizing the proportionality between $\ln[f(\theta)\Delta n/A\theta]$ and R. The values of C and Y vary with annealing conditions (temperature and time).

In evaluating the orientation function for partially oriented aggregate, $\langle P_2(\theta)\rangle$ is defined by Ward[18] by the following equation:

$$\langle P_2(\theta)\rangle = \Delta n_a/\Delta n_{\max} \qquad (13)$$

which is the same function named by Hermans.[15]

So if θ is the angle made between the principal axis of a statistical segment of such a fiber and the stretching direction, the orientation function may be defined as $f(\theta)$, and the birefringence is then given by[19]

$$\Delta n_a = (\alpha_{\parallel} - \alpha_{\perp})f(\theta) \qquad (14)$$

where $(\alpha_{\parallel} - \alpha_{\perp})$ is the difference between the principal polarizabilities of the statistical segment.

The Kuhn–Treloar-type theory gives for $f(\theta)$,

$$f(\theta) = (\tfrac{2}{5})N_c(DR^2 - 1/DR) \qquad (15)$$

where N_c is the number of chains per unit volume and depends on the number of crystallinites in the polymer material.

Table III Values of N for PET Fiber

Annealing Temperature	N
120°C	3.5
140°C at 2 h	3.6
160°C	3.3
120°C	2.5
140°C at 4 h	5.9
160°C	2.8

It can be shown[6] that the orientation function for the random links as observed previously is given by

$$[P_2(\theta)] = (DR^2 - DR^{-1})/5N \qquad (16)$$

where N is the number of random links between the network junction points (the entanglements), and DR is the extension or draw ratio. The value of N for PET fiber is given in Table III.

EXPERIMENTAL PROCEDURE: RESULTS AND DISCUSSION

Sample Preparation and Annealing

The polyester fibers were distributed in a cocoon form on a glass rods with free ends, which were then heated in an electric oven whose temperature was adjusted to be at different temperature (120, 140, and 160 ± 1°C). Hence, the samples were annealed for the annealing times (2 and 4 h), then left to cool in air at room temperature 28 ± 1°C.

Double Beam Inteferometry

A Pluta polarizing interference microscope[8,9] was connected to a device to dynamically study the draw ratio. The totally duplicated image of the fiber was used to calculate the mean refractive indices $n_a^{\parallel}$ and $n_a^{\perp}$ and the birefringence Δn_a of polyester fibers at different draw ratios with different conditions of annealing. The values of $n_a^{\parallel}$, $n_a^{\perp}$, and Δn_a for PET fiber are given in Table II(a)–(f).

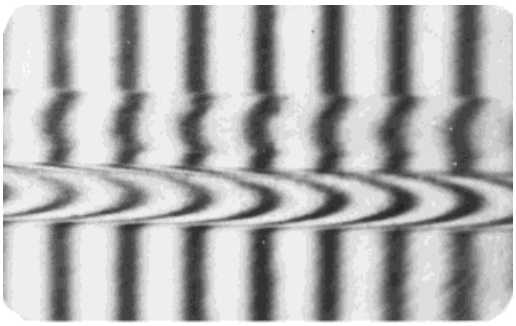

(a)

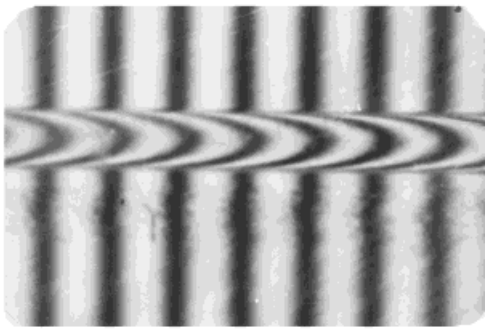

(b)

Plate 1 (a)–(b): The microinterferogram of a totally duplicated image of undrawn PET fiber unannealed (parallel and perpendicular) is given. Monochromatic light of $\lambda = 546$ nm was used.

Plate 1(a)–(b) shows a microinterferogram of totally duplicated images of undrawn polyester fiber using the Pluta microscope with monochromatic light of wavelength 546 nm, in parallel and perpendicular directions, respectively. The refractive index of the immersion liquid was selected to allow the fringe shift to be small.

Plates 2(a)–(f) and 3(a)–(f) are microinterferograms of the totally duplicated images in parallel and perpendicular direction, respectively, of polyester fibers samples annealed at different temperatures (120, 140, and 160 ± 1°C) and two times (2 and 4 h). Monochromatic light of wavelength 546 nm was used. In plates 2(a)–(f) and 3(a)–(f), the immersion liquid was selected to allow the fringe shift to be small (within one to two orders of interference) and to determine accurately the point of connection of the fringe in the liquid and fiber regions. Plates 2(a)–(f) and 3(a)–(f) also show that the fringe shift increases as the draw ratio increases and the diameter of the fiber decreases. The refractive index of the immersion liquid were 1.658 and 1.569 at 18°C, for parallel and perpendicular directions, respectively. Using these interferograms and eqs. 1(a) and 1(b), the mean refractive index of the parallel and perpendicular directions with different draw ratios at different annealing conditions was calculated.

Figure 1(a)–(b) shows the variation of the crystallinity and $(1 - \chi)$ of unannealing polyester fibers due to the changing draw ratio.

The apparent volume fraction (χ) of crystallinity was calculated from eq. (7) using the calculated density values. The results are given in Table II(a)–(f) and plotted in Figure 2(a)–(f), which shows the variation of the crystallinity of polyester fibers due to the changing draw ratio at different annealing conditions (annealing temperatures are 120, 140, and 160 ± 1°C; annealing times are 2 and 4 h). It is quite obvious that the crystallinity is lower for undrawn fibers than for drawn samples. The value of χ, increases and then decreases with increasing draw ratio.

Figure 3(a)–(f) shows the variation of the $(1 - \chi)$ of polyester fibers due to changing draw ratio at different annealing conditions (annealing temperatures are 120, 140, and 160 ± 1°C; annealing times are 2 and 4 h).

Figure 4(a) and (c) shows the variation of the number of chains per unit volume N_c of polyester fibers due to the changing draw ratio at different annealing conditions (annealing temperatures are 120, 140, and 160 ± 1°C; annealing times are 2 and 4 h).

Figure 5(a) and (b) shows the relationship between optical orientation (f_θ) from eq. (10) of polyester fibers from the duplicated image as a function of the draw ratio at different annealing conditions (annealing temperatures are 120, 140, and 160 ± 1°C; annealing times are 2 and 4 h).

Figure 6(a) and (b) shows the relationship between $(\Phi^{\parallel} - \Phi^{\perp})/(\Phi^{\parallel} + 2\Phi^{\perp})$ and the draw ratio and gives an increase in $(\Phi^{\parallel} - \Phi^{\perp})/(\Phi^{\parallel} + 2\Phi^{\perp})$ as the draw ratio increases. These results indicate that drawing process of PET fibers causes changes in the alignment of polymeric chains.

Figure 7(a) and (b) shows the angle of orientation as a function of the draw ratio at different annealing conditions (annealing temperatures are 120, 140, and 160 ± 1°C; annealing times are 2 and 4 h).

Figure 8(a)–(f) shows the relationship be-

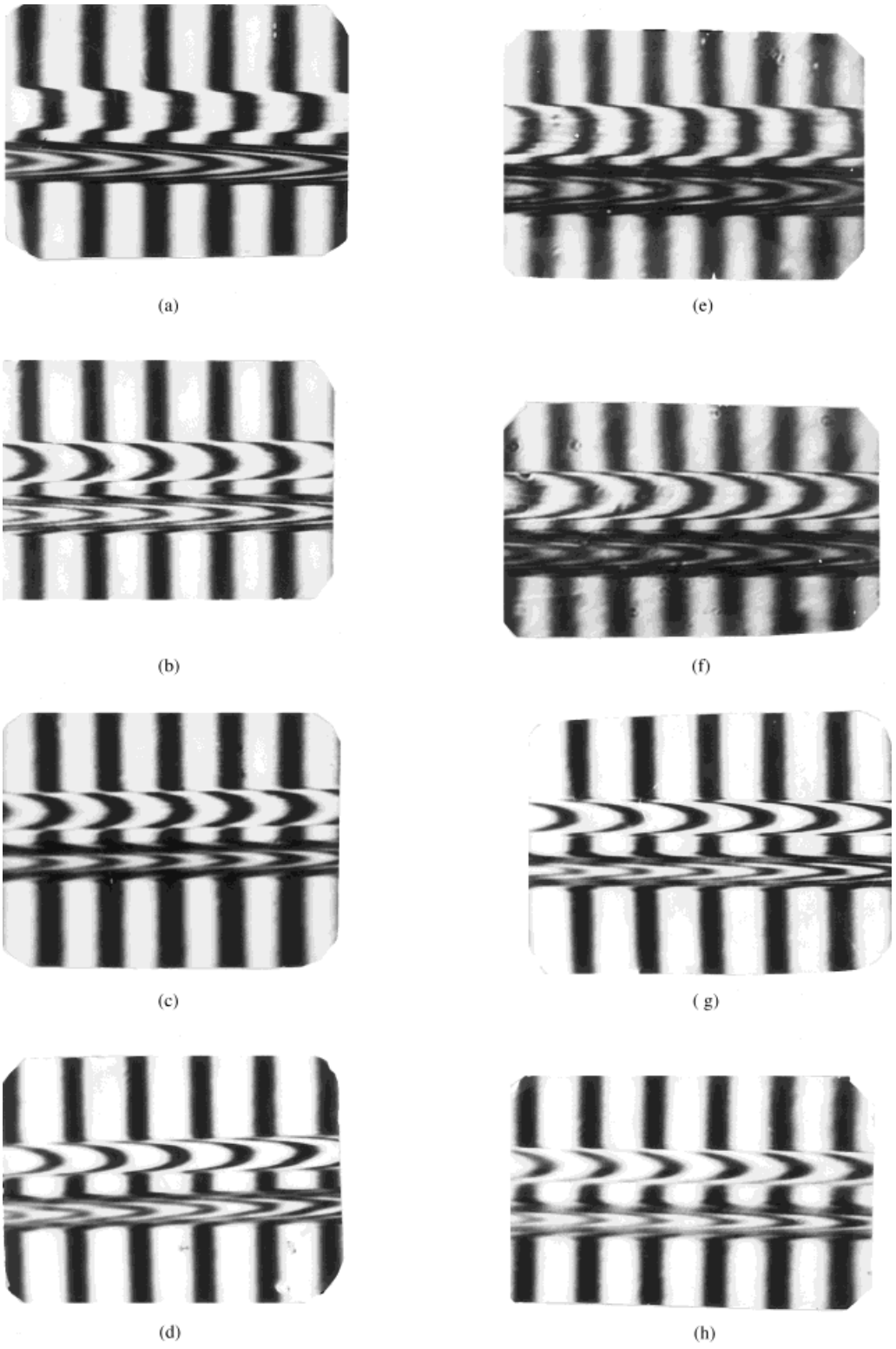

Plate 2 (a)–(f): The microinterferograms of a totally duplicated image of polyester fiber, which was annealed at different temperatures (120, 140, and 160 ± 1°C at two constant times of 2 and 4 h) with different draw ratios (parallel). Monochromatic light of $\lambda = 546$ nm was used.

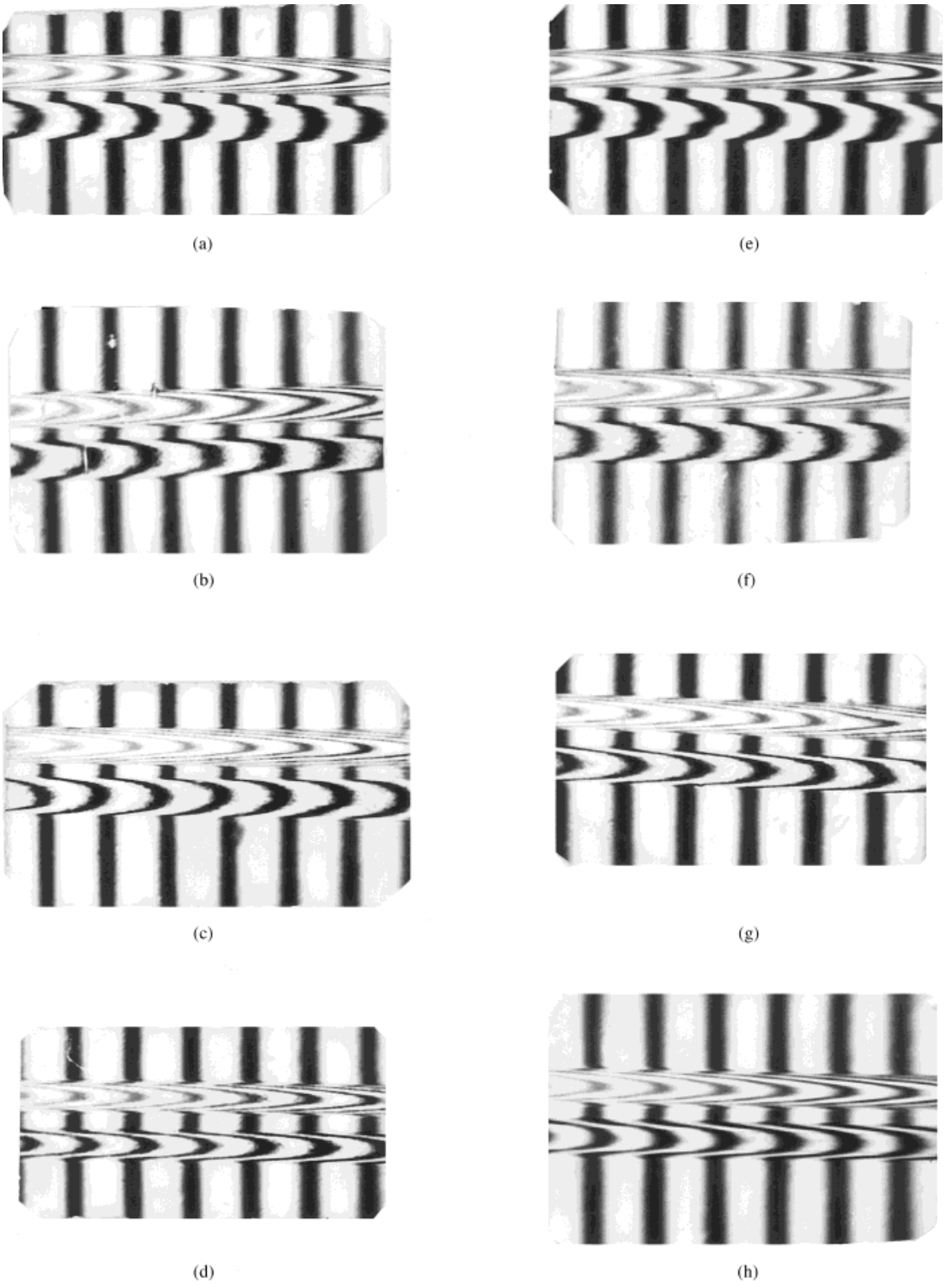

Plate 3 The microinterferograms of a totally duplicated image of polyester fiber, which was annealed at different temperatures (120, 140, and 160 ± 1°C at two constant times of 2 and 4 h) with different draw ratios (perpendicular). Monochromatic light of $\lambda = 546$ nm was used.

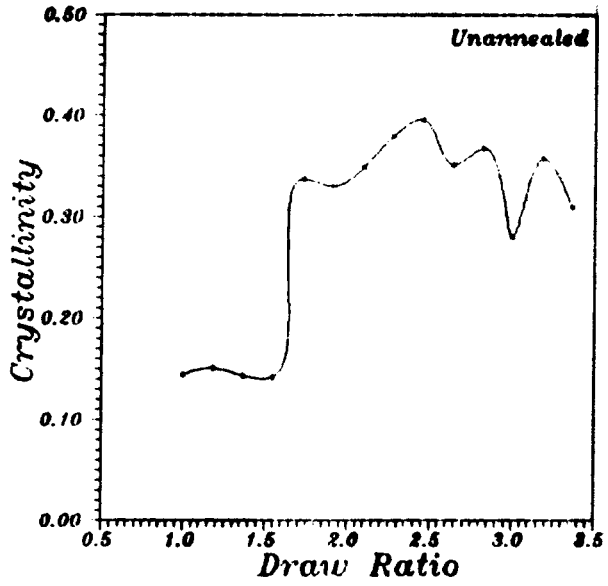

(a)

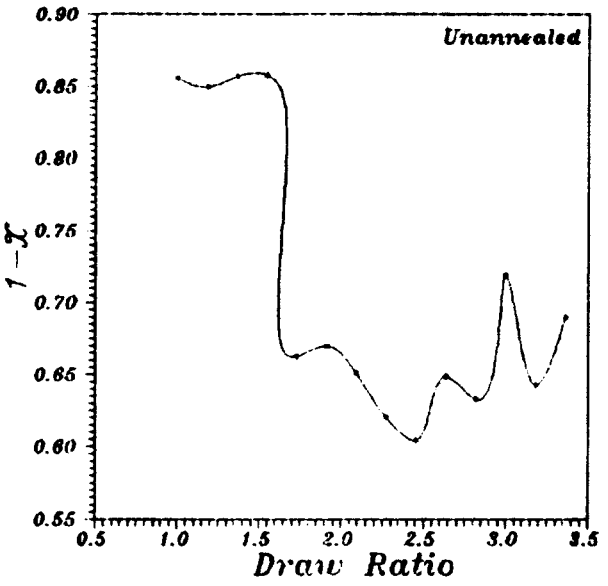

(b)

Figure 1 (a) and (b): The relationship between the draw ratio with crystallinity χ and $(1 - \chi)$ of unannealed PET fiber.

tween the optical orientation function $\langle P_2(\theta)\rangle$ and the value $(\Phi^{\parallel} - \Phi^{\perp})/(\Phi^{\parallel} + 2\Phi^{\perp})$; it gives a straight line. The slope of this straight line gives the constant $(\Delta\alpha/3\alpha_o)$ for PET fibers, which was found to be 0.104.

Figure 9(a)–(b) shows the relationshipe between $\ln[f(\theta)\Delta n/A\theta]$ and the draw ratio at different annealing conditions (annealing temperatures are 120, 140, and 160 ± 1°C; annealing times are 2 and 4 h).

CONCLUSION

From the measurements and calculations relating the change of optical properties to the thermal annealing process for polyester fibers, the following conclusions may be drawn.

1. An empirical formula is suggested to relate the variation of the cross sectional area, angle of orientation, orientation factor, and birefringence of PET fibers with the draw ratio.
2. The microinterferograms clearly to identify differences in optical path variations due to different drawing processes at different annealing conditions.
3. The higher the orientation, the more mutually parallel the molecules and the smaller the average angle formed by them with the fiber axis.
4. The orientation angle decreases with increasing draw ratio at different annealing condition.
5. The study of change of $n_a^{\parallel}$, $n_a^{\perp}$, and Δn_a with respect to the annealing and drawing processes, clarifies that the isothermal properties of the structure in perpendicular direction to the fiber axis differ from those in an axial direction, which is expected for an anisotropy medium.
6. As $n_a^{\parallel}$ increases, i.e., the process of axial orientation increases crystallinity by orienting the molecules.
7. Annealing the fibrous structure, however, affects the diffusion properties.
8. The effects of the annealing process on polyester fibers depends on the time and temperature of annealing.
9. Changes in the isotropic refractive indices n_{iso} is related to the degree of order and crystallinity of the fiber, as well as the density of sample $[(n_{iso} - 1)/\rho] = K$.
10. The results shown in Table II(a)–(f) indicate that the constant K varies with the draw ratio at different annealing conditions.
11. It is found that increasing the draw ratio at different annealing temperatures and times gives an increase in the optical orientation function [Fig. 9(a)–(f)], while the

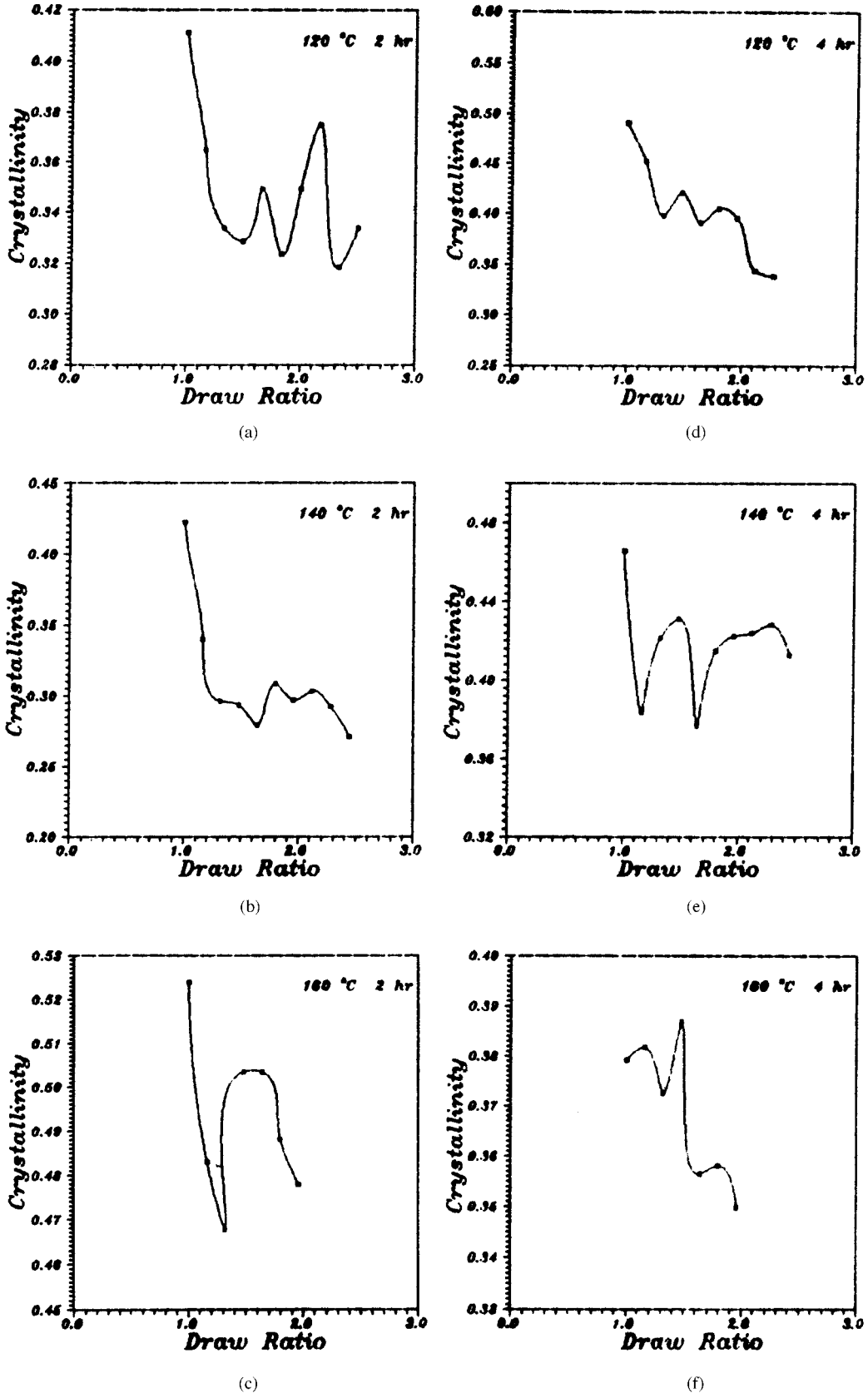

Figure 2 (a)–(f): The relationship between the draw ratio and crystallinity χ of PET fiber at different annealing conditions (120, 140, and 160°C at two constant times of 2 and 4 h).

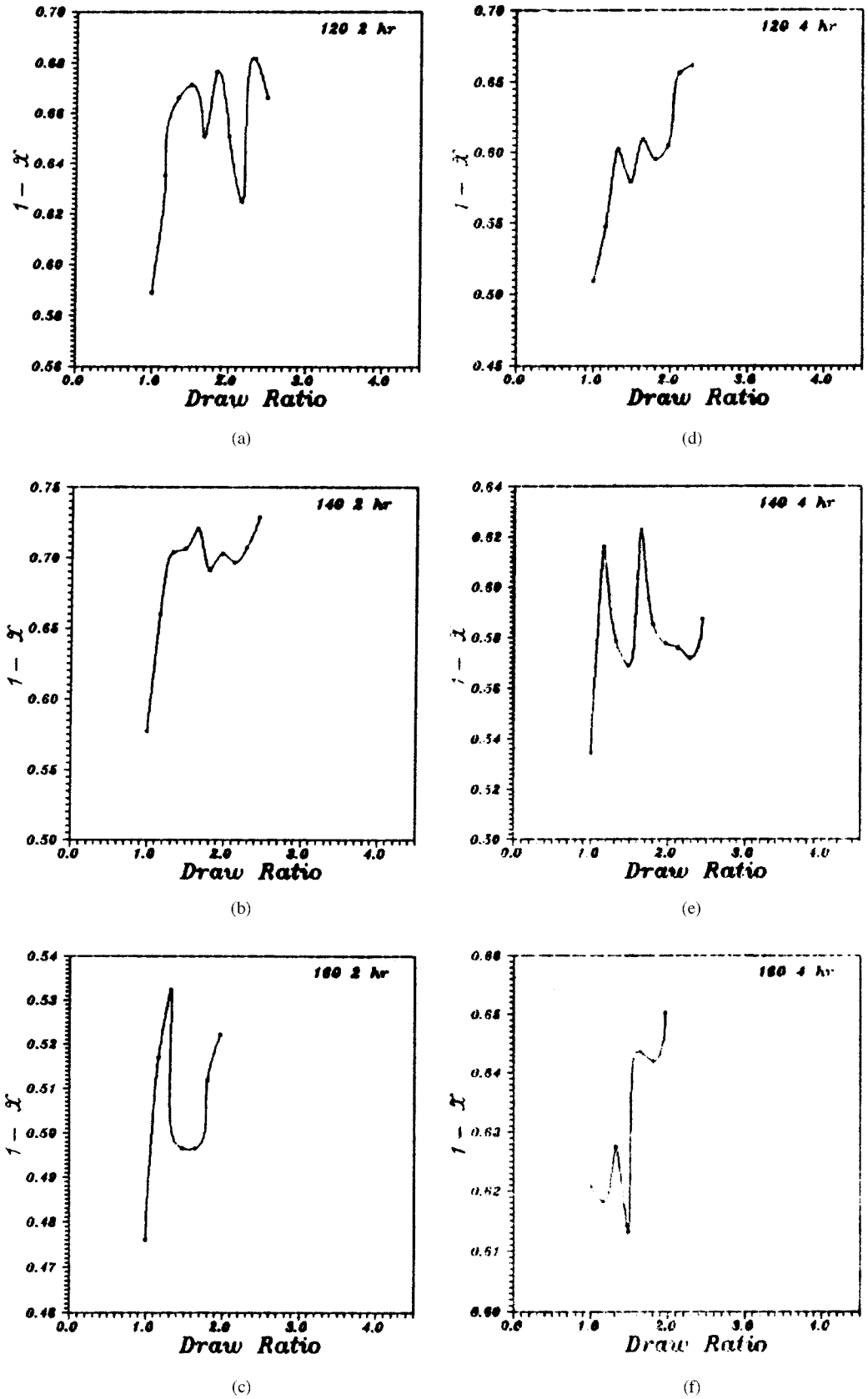

Figure 3 (a)–(f): The relationship between the draw ratio and $(1 - \chi)$ of PET fiber at different annealing conditions (120, 140, and 160°C at two constant times of 2 and 4 h).

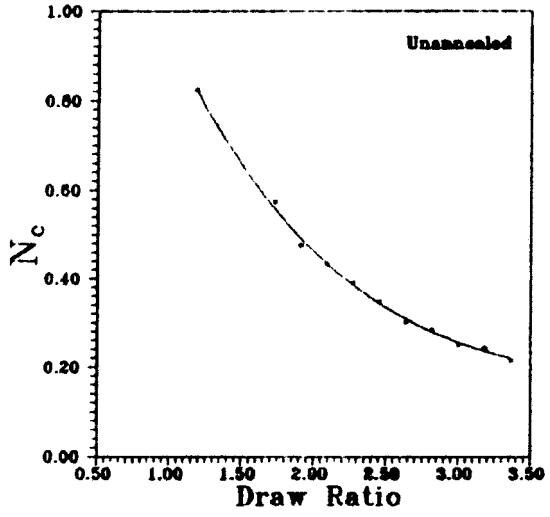

(a)

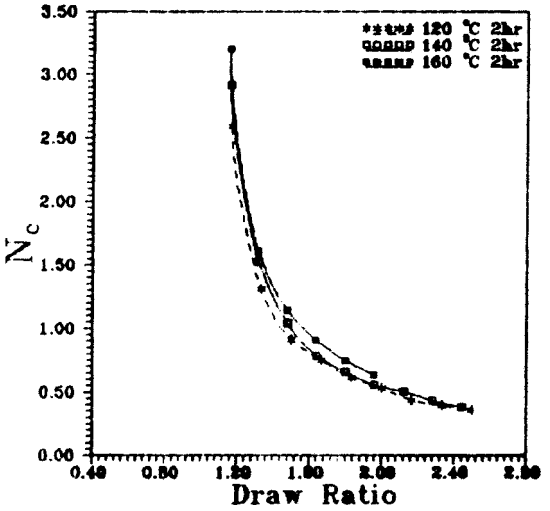

(b)

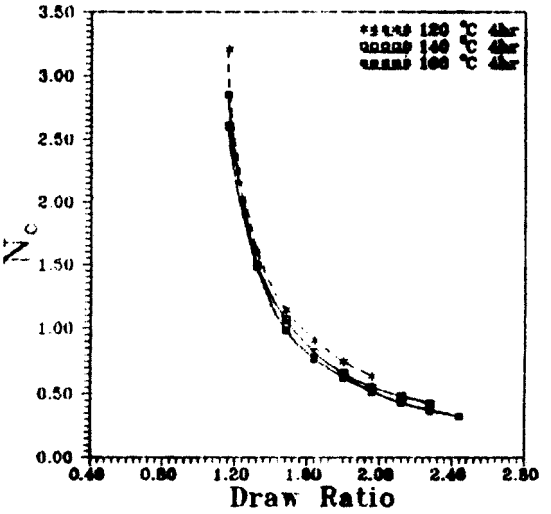

(c)

Figure 4 (a)–(c): The relationship between the draw ratio and number of chains per unit volume N_c of PET fiber at different annealing conditions (120, 140, and 160°C at two constant times of 2 and 4 h).

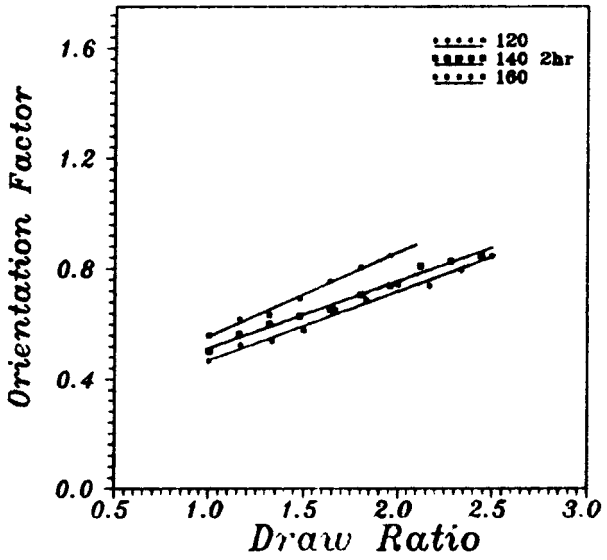

(a)

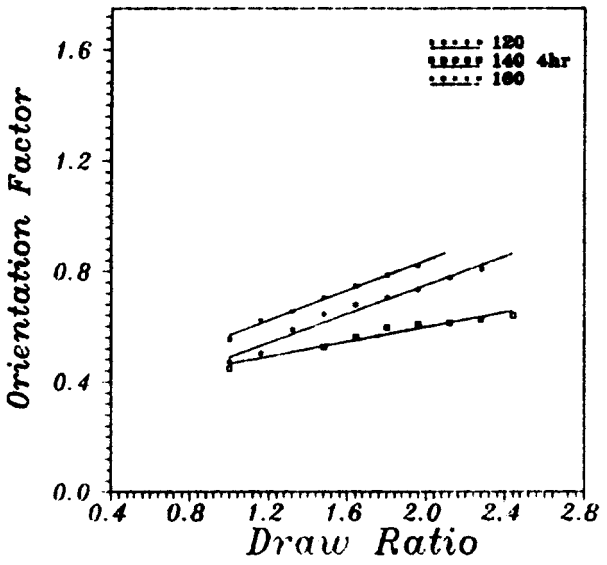

(b)

Figure 5 (a) and (b): The relationship between the optical orientation function f_θ and the draw ratio of PET fiber at different annealing conditions (120, 140, and 160°C at two constant times of 2 and 4 h).

value ($\Delta\alpha/3\alpha_o$), which depends upon the molecular structure, remains constant.

12. Study of the density variations due to drawing indicates the mass redistribution associated with the drawing process of polyester fibers.
13. The annealing process affects other physical properties (thermal, electrical, elastic, etc.) of polyester, as well as its optical properties. Further studies should be carried out in order to detect which properties are improved by annealing.

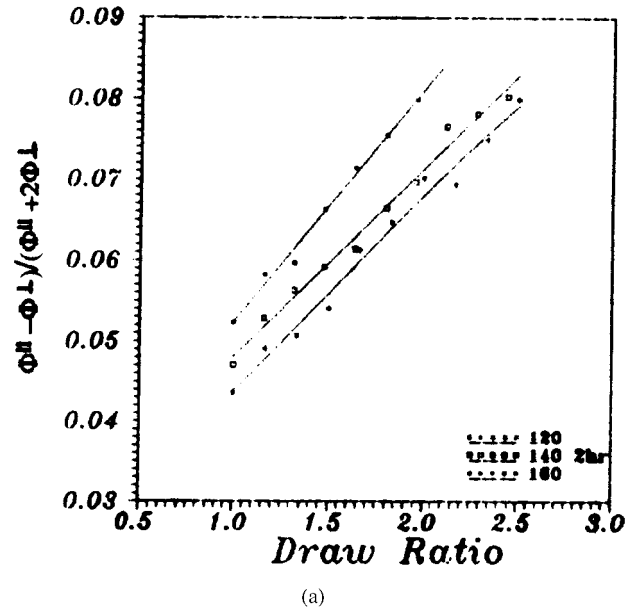

(a)

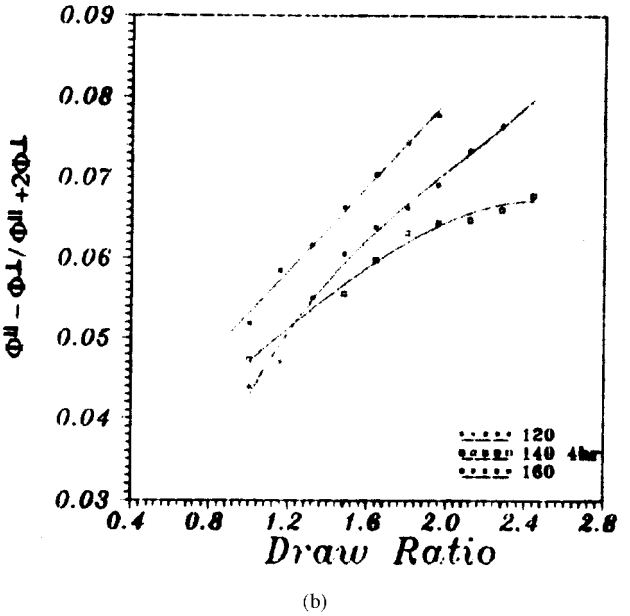

(b)

Figure 6 (a) and (b): The relationship between $(\Phi^{\parallel} - \Phi^{\perp})/(\Phi^{\parallel} + 2\Phi^{\perp})$ and the draw ratio of PET fiber at different annealing condition (120, 140, and 160°C at two constant times of 2 and 4 h).

14. Evaluation of crystallinity with the draw ratio decreased at first in all different annealing conditions, which indicates a regrouping due to mobilities of chain units of polyester fiber during the drawing process.
15. Thermal annealing can provide supplementary information on the sturactural features related to the thermal performance of materials, where the variation of specific volume is related to crystallinity, density, and mass redistribution of the sample.

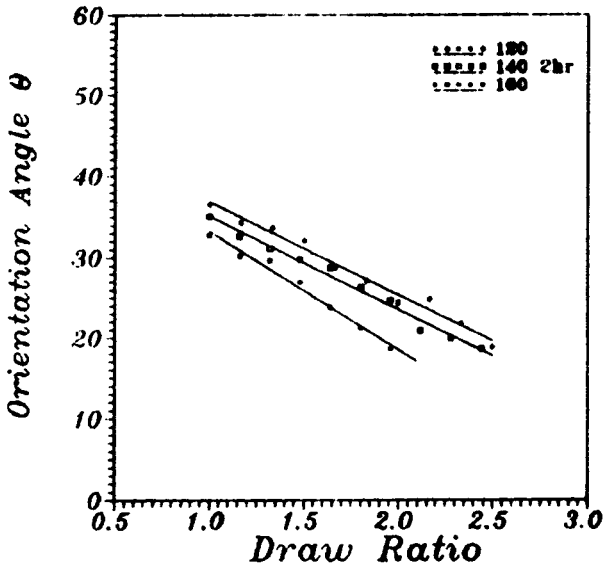

(a)

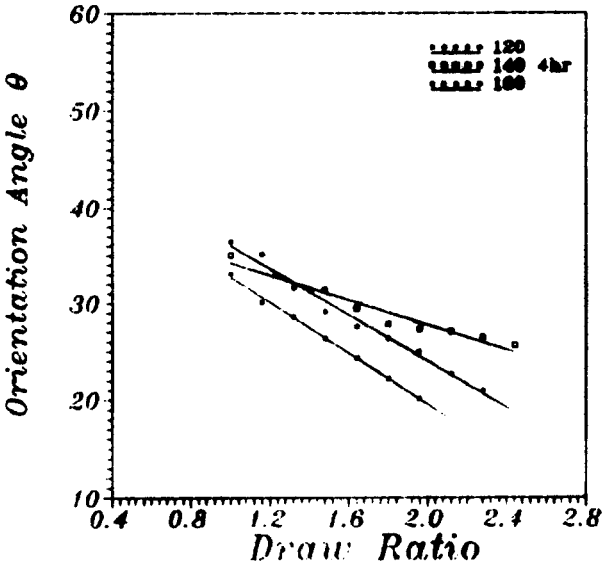

(b)

Figure 7 (a) and (b): The angle of orientation (θ) as function of the draw ratio of PET fiber at different annealing conditions (120, 140, and 160°C at two constant times of 2 and 4 h).

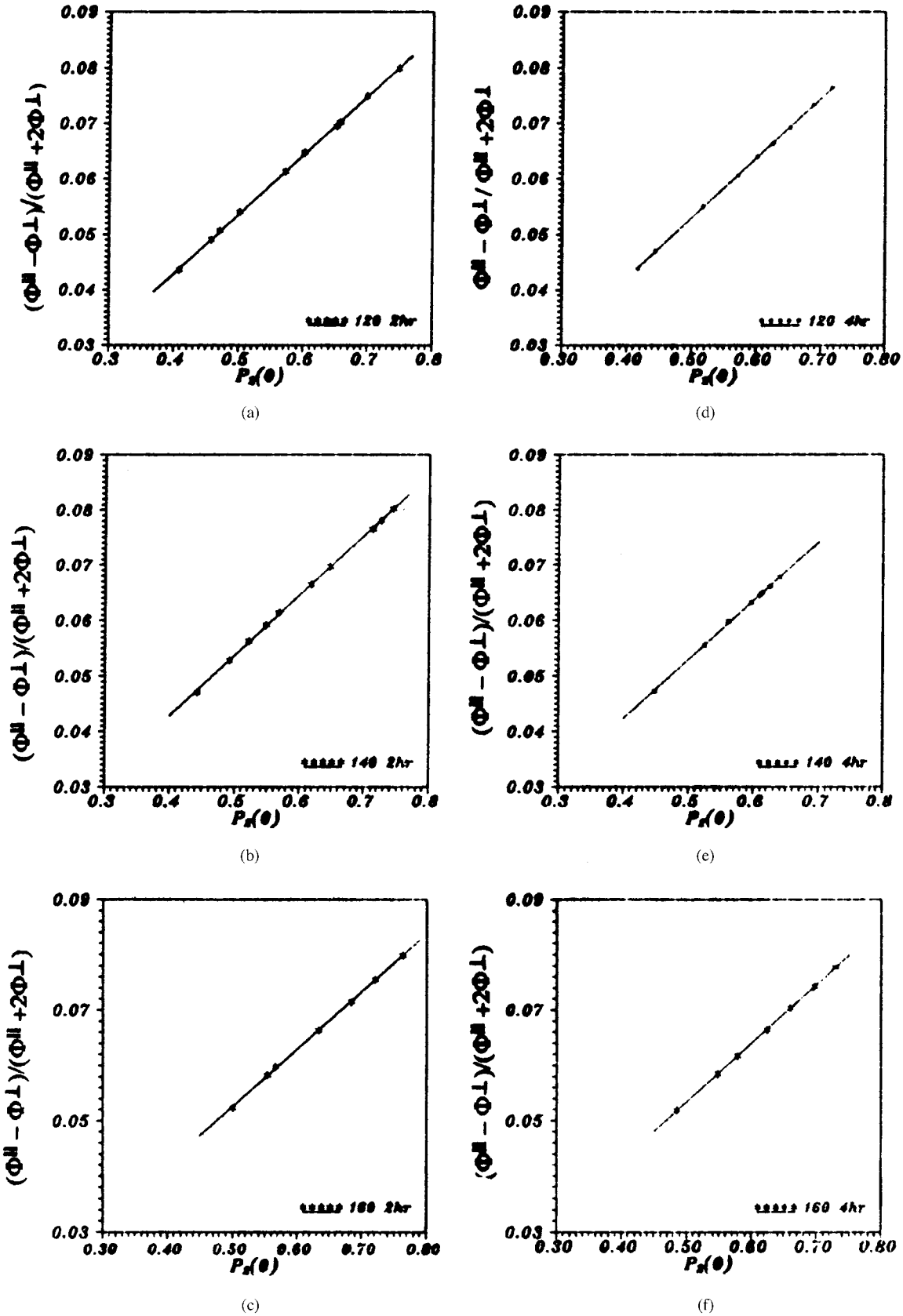

Figure 8 (a)–(f): The relationship between the optical orientation function $\langle P_2(\theta) \rangle$ and the value $\{\Phi^{\parallel} - \Phi^{\perp}/\Phi^{\parallel} + 2\Phi^{\perp}\}$ of drawing PET fiber at different annealing conditions (120, 140, and 160°C at two constant times of 2 and 4 h).

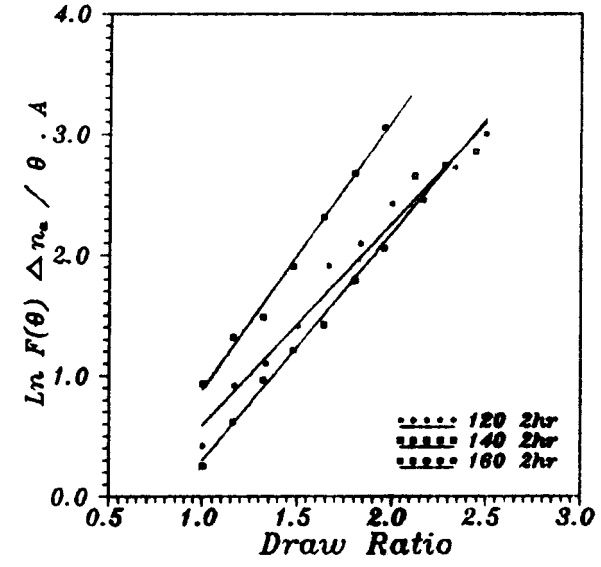

(a)

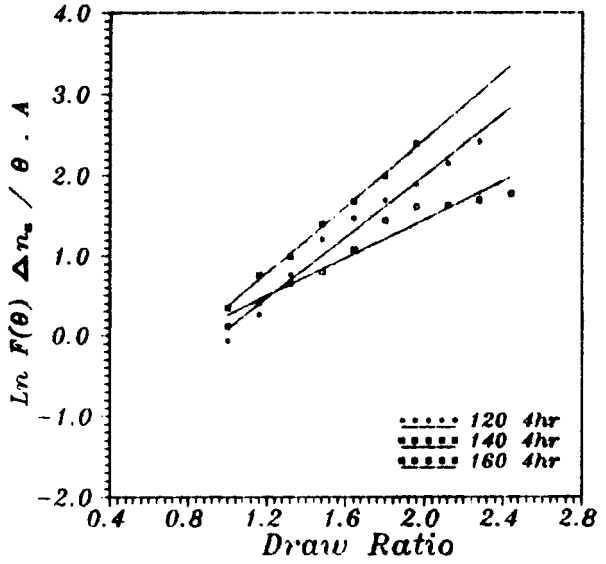

(b)

Figure 9 (a) and (b): The relationship between $\ln[f(\theta)\Delta n/A\theta]$ and the draw ratio of PET fiber at different annealing conditions (120, 140, and 160°C at two constant times of 2 and 4 h).

In conclusion, the structural orientation changes due to the annealing and drawing processes, as observed by both two-beam techniques, is very promising; and further study is required in areas which have not yet been explored. Since $n_a^{\parallel}$, $n_a^{\perp}$, Δn_a, and n_{iso} are a consequence of the material annealed, reorientation of PET fibers may occur not only during fabrication but also after the fabrication process.

REFERENCES

1. A. Bendak and S. M. El-Marasfi, *Bull. NRC Egypt,* **16,** 165 (1991).
2. I. M. Fouda, M. M. El-Tonsy, and A. H. Oraby, *J. Mat. Sci.,* **25,** 1416 (1990).
3. A. A. Hamza, I. M. Fouda, K. A. El-Farahaty, and E. A. Seisa, *Polym. Test.,* **10,** 195 (1991).
4. A. A. Hamza, I. M. Fouda, M. M. El-Tonsy, and F. M. El-Sharkawy, *J. Appl. Polym. Sci.,* **56,** 1355 (1995).
5. H. M. Heuvel, L. J. Lucas, C. J. M. Van Den Hevl, and A. P. De Weijer, *J. Appl. Polym. Sci.,* **45,** 1649 (1992).
6. J. M. Perena, R. A. Duckett, and I. M. Ward, *J. Appl. Polym. Sci.,* **25,** 1381 (1980).
7. A. Keller, *J. Polym. Sci.,* **21,** 363 (1956).
8. M. Pluta, *J. Optica Acta,* **18** 661 (1971).
9. M. Pluta, *J. Microsc.,* **96,** 309 (1972).
10. J. R. Samuels, *Structured Polymer Properties,* Wiley, New York, 1974, p. 51.
11. G. L. Bourvellec and J. Beautemps, *J. Appl. Polym. Sci.,* **39,** 329 (1990).
12. A. J. de Vries, C. Bonnebat, and J. Beautemps, *J. Polym. Sci., Polym. Symp.,* **5,** (1977).
13. I. M. Ward, *Structured and Properties of Oriented Polymers,* Applied Science, London, 1975, p. 57.
14. E. W. Fischer and S. Fakirov, *J. Mat. Sci.,* **11,** 1041 (1976).
15. P. H. Hermans, *Contributions to the Physics of Cellulose Fibers,* North Holland, Amsterdam, 1946.
16. J. S. Foot and I. M. Ward, *J. Mat. Sci.,* **10,** 955 (1975).
17. I. M. Ward, *Proc. Phys. Soc. London,* **80,** 1176 (1962).
18. I. M. Ward, *J. Polym. Sci., Polym. Symp.,* **58,** 1 (1977).
19. R. S. Stein, *J. Polym. Sci., Polym. Symp.,* **34,** 709 (1959).